

# Chiral phase transition at 180° domain walls in ferroelectric PbTiO<sub>3</sub> driven by epitaxial compressive strains

Yu-Jia Wang, Yin-Lian Zhu, and Xiu-Liang Ma

Citation: *Journal of Applied Physics* **122**, 134104 (2017); doi: 10.1063/1.5006607

View online: <http://dx.doi.org/10.1063/1.5006607>

View Table of Contents: <http://aip.scitation.org/toc/jap/122/13>

Published by the *American Institute of Physics*

---

## Articles you may be interested in

[Electric-field control of electronic transport properties and enhanced magnetoresistance in La<sub>0.7</sub>Sr<sub>0.3</sub>MnO<sub>3</sub>/0.5BaZr<sub>0.2</sub>Ti<sub>0.8</sub>O<sub>3</sub>-0.5Ba<sub>0.7</sub>Ca<sub>0.3</sub>TiO<sub>3</sub> lead-free multiferroic structures](#)

*Journal of Applied Physics* **122**, 134102 (2017); 10.1063/1.4990513

[Effect of Holmium substitution on the magnetic and magnetodielectric properties of multiferroic Bi<sub>2</sub>Fe<sub>4</sub>O<sub>9</sub>](#)

*Journal of Applied Physics* **122**, 134103 (2017); 10.1063/1.4994645

[New functionalities of potassium tantalate niobate deflectors enabled by the coexistence of pre-injected space charge and composition gradient](#)

*Journal of Applied Physics* **122**, 133111 (2017); 10.1063/1.4996732

[Crystal orientation-dependent mechanical property and structural phase transition of monolayer molybdenum disulfide](#)

*Journal of Applied Physics* **122**, 135105 (2017); 10.1063/1.4996941

[Multiferroic properties of the Y<sub>2</sub>BiFe<sub>5</sub>O<sub>12</sub> garnet](#)

*Journal of Applied Physics* **122**, 134101 (2017); 10.1063/1.5005908

[Solid-phase epitaxial film growth and optical properties of a ferroelectric oxide, Sr<sub>2</sub>Nb<sub>2</sub>O<sub>7</sub>](#)

*Journal of Applied Physics* **122**, 135305 (2017); 10.1063/1.4997813

---

**Scilight**

Sharp, quick summaries **illuminating**  
the latest physics research

Sign up for **FREE!**

**AIP**  
Publishing

# Chiral phase transition at 180° domain walls in ferroelectric PbTiO<sub>3</sub> driven by epitaxial compressive strains

Yu-Jia Wang,<sup>1</sup> Yin-Lian Zhu,<sup>1</sup> and Xiu-Liang Ma<sup>1,2,a)</sup>

<sup>1</sup>Shenyang National Laboratory for Materials Science, Institute of Metal Research, Chinese Academy of Sciences, Wenhua Road 72, 110016 Shenyang, China

<sup>2</sup>School of Materials Science and Engineering, Lanzhou University of Technology, Langongping Road 287, 730050 Lanzhou, China

(Received 18 April 2017; accepted 25 September 2017; published online 4 October 2017)

Chiral ferroelectric domain walls are theoretically predicted to be promising in novel electronic memory devices. In order to develop a chirality-based device, understanding the chiral phase transition is of great importance for chirality manipulation. In this work, we systematically studied the chiral phase transition at 180° domain walls in ferroelectric PbTiO<sub>3</sub> (PTO) under epitaxial compressive strains by first principles calculations. It is found that with the increase of the compressive strain, the Bloch components decrease due to the coupling of polarization and strain, while the components normal to domain walls increase because of the large stress gradients. The domain wall changes from a mixed Ising-Bloch type to the Ising type. It is also found that the domain wall energy increases with the increment of compressive strain, indicating that the spacings of 180° domain walls would be large for the highly compressed PTO films. These findings may provide useful information for the development of novel ferroelectric devices. *Published by AIP Publishing.*

<https://doi.org/10.1063/1.5006607>

## I. INTRODUCTION

Domain walls (DWs) are the physical separations between regions with uniform order parameters (domains). Several theoretical and experimental studies show that they actually possess abundant internal structures and novel functionalities. For example, ferroelastic DWs in incipient ferroelectrics SrTiO<sub>3</sub> (Refs. 1 and 2) and CaTiO<sub>3</sub>,<sup>3,4</sup> as well as antiphase DWs in antiferroelectric PbZrO<sub>3</sub> (Ref. 5), are found to be polar. These polar DWs are bi-stable in nature, which means that they can be switched by external electric fields and used as high-density memory devices.

In ferroelectrics, 180° DWs were traditionally thought to be of Ising-type: the polarization vectors only change magnitudes but do not rotate around DWs.<sup>6,7</sup> However, recent theoretical studies indicate that polarization vectors actually rotate around DWs, and other polarization components may exist around DWs, including those normal and parallel to DWs.<sup>8–16</sup> The components parallel to DWs are termed as Bloch-type and there exist two chiral variants according to the rotation manner of polarization vectors, while the normal components are termed as Néel-type, and this type of DWs is not chiral as there exists a mirror symmetry.<sup>17</sup> 180° DWs in PbTiO<sub>3</sub> (PTO) were predicted to undergo a ferroelectric transition to develop large Bloch-type polarization components with the decrease of temperature.<sup>18</sup> Although tail-to-tail polarization components normal to DWs also exist around 180° DWs in PTO due to the flexoelectricity, these components are extremely small and become exactly zero at the DW center. Therefore, 180° DWs in PTO should not be considered as Néel-type according to the classification proposed by Hlinka *et al.*<sup>17</sup>

Epitaxial strain is a powerful tool to manipulate the properties of ferroelectrics. The Curie temperature, polarization magnitude and domain structures could be modified by applying different epitaxial strains to ferroelectric films.<sup>19–22</sup> However, the effect of epitaxial strain on the chirality of DWs has been poorly studied. Previously, Stepkova *et al.* used phase-field simulations to predict a phase transition from Bloch-like to Ising-like 180° DWs in rhombohedral BaTiO<sub>3</sub> by applying a compressive epitaxial stress.<sup>11</sup> Their following work showed that the dielectric permittivity would diverge at the transition point.<sup>23</sup> Here, we studied the effect of epitaxial strain on the chirality of 180° DWs in PTO, a prototype of tetragonal ferroelectrics. We found that the Bloch components decrease with increasing compressive strain, resulting in a chiral phase transition around 180° DWs from the mixed Ising-Bloch to the Ising type. In contrast, the normal components increase due to large stress gradients.

## II. METHODS

All the calculations were performed using the VASP code.<sup>24–26</sup> The local density approximation (LDA) exchange-correlation functional was used with the projector-augmented wave (PAW) method.<sup>27</sup> The plane wave cutoff energy was 550 eV. The O 2s2p, Ti 3s3p3d4s, and Pb 5d6s6p electrons were treated as the valence electrons. The optimized lattice parameters of *a* and *c* for PTO are 3.867 Å and 4.033 Å, respectively, consistent with previous calculation results.<sup>9,28</sup> The experimental lattice parameters of PTO are *a* = 3.905 Å and *c* = 4.152 Å,<sup>29</sup> i.e., they were underestimated by 1% and 3%, respectively. We set the lattice parameters of the PTO unit cell to the experimental and theoretical values separately and calculated their polarizations by the Berry-phase method.<sup>30</sup> The results are  $P_{\text{expt}} = 94 \mu\text{C}/\text{cm}^2$  and  $P_{\text{theo}} = 78 \mu\text{C}/\text{cm}^2$ ,

<sup>a)</sup>Author to whom correspondence should be addressed: xлма@imr.ac.cn

respectively. That is to say, the underestimation of lattice parameters results in a polarization difference of 17%. If we assume that the domain wall energy is proportional to the square of the polarization gradient at the domain wall center, we may say that the domain wall energy might be underestimated by 31%.

The [100]-oriented 180° DW was considered and a  $12 \times 1 \times 1$  supercell was chosen, since our previous studies showed that this size would be large enough to reflect the polarization state of 180° DWs.<sup>16</sup> The Ising, Bloch and normal components are the polarization components along the  $z$ ,  $y$  and  $x$  directions, as shown in Fig. 1. The structure relaxations were considered to converge when the force on each atom is less than 2 meV/Å. We used the Born effective charge and the atomic displacements of each atom to calculate the polarization of each unit cell. We chose two types of unit cells, whose central planes are the TiO<sub>2</sub> and PbO planes, respectively.<sup>7,9</sup>

To compare the stability of DW models with different chiralities, we first studied the Ising-type DW models (DW-I). As reported in our previous studies, Ising-type polarization components are the main feature of 180° DWs in PTO and the emergence of Bloch-type and normal components will only cause about 10% reduction of the DW energy.<sup>16</sup> We applied compressive epitaxial strains to  $a$  and  $b$  axes of DW-I models and allowed the  $c$  axis to relax in order to obtain the optimized DW-I models. Using these models as references, we did constrained relaxations to determine the optimized Bloch and normal components at different strains. The normal components can be obtained by direct relaxation under the constraint imposed by the symmetry of the mirror plane normal to the  $y$  axis. The DW model containing normal components is named as DW-IN.

The determination of optimized Bloch components is more difficult: One has to push the Pb atoms at DW centers to a series of distances along the  $y$  axis and find the energy minimum along this path, while the  $x$  coordinates are fixed. The pushing of Pb atoms is marked by arrows in the atomic models in Fig. 1. After these steps, the mixed Ising-Bloch-type DW models were obtained (DW-IB). Full relaxations based on these models result in the emergence of normal components (DW-IBN).

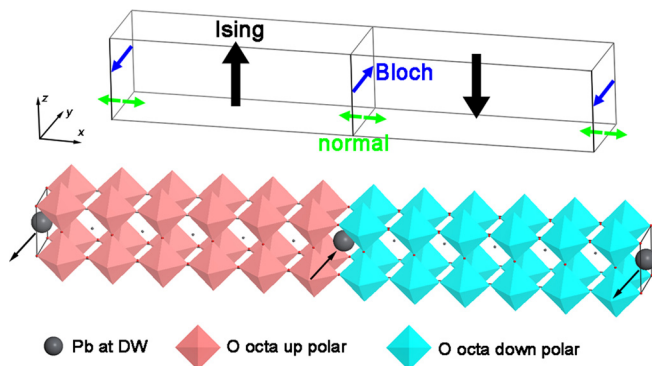


FIG. 1. The schematic diagram (up panel) and the atomic model (down panel) of 180° DWs in PTO. The Ising, Bloch and normal components are marked as black, blue and green arrows. In the atomic model, the oxygen octahedra with up and down polarizations are colored red and blue, and the pushing of Pb atoms is marked by arrows.

The domain wall energies were calculated according to the equation

$$E_{dw} = (E_{tot}^{dw} - E_{tot}^{bulk})/2S, \quad (1)$$

where  $E_{tot}^{dw}$  is the total energy of the system containing 180° DWs,  $E_{tot}^{bulk}$  is the total energy of the equivalent system without 180° DWs, and  $S$  is the DW area.

### III. RESULTS AND DISCUSSION

#### A. DW energies for different types of 180° DW models

Figure 2 gives the results of DW energies as the function of compressive strain for four DW models. It is found that the DW energy increases with the increase of compressive strain, which means that the density of DWs would decrease for films with large compressive strains. At zero strain, the emergence of Bloch and normal components could reduce the DW energy. As the strain goes left further, the DW energy difference between DW-I (black) and DW-IB (red) becomes marginal and at the strain states of  $-1.5\%$  and  $-2\%$ , the bars of DW-IB (red) and DW-IBN (green) disappear. As to be shown in Section III B, the DW models with Bloch components become unstable at these strain states.

Another thing worthy to mention is that the DW energies obtained under the condition of relaxing the  $c$  axis are lower than those under the condition of fixing the  $c$  axis. For example, at zero strain, the DW energy of DW-I in the case of fixing the  $c$  axis is 130 mJ/m<sup>2</sup>,<sup>16</sup> (marked as a star in Fig. 2), while that in the case of relaxing the  $c$  axis is only 108 mJ/m<sup>2</sup>, nearly 20% reduction. The reason can be understood as follows: During the process of relaxing the  $c$  axis, the total energy of the DW model decreases, while the bulk term increases due to the reduced lattice parameter  $c$ . As a result, the DW energy reduces.

#### B. The evolution of polarization components with strains

Figure 3 gives the DW energy difference of the DW-IB and DW-I models as the Pb atoms at DW planes are pushed along the  $y$  axis at different compressive strains. It can be found that there are potential wells at the positions of zero

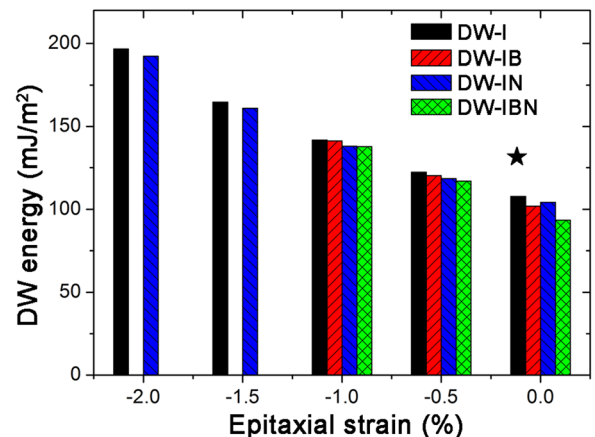


FIG. 2. The DW energies of different models at different epitaxial strains.

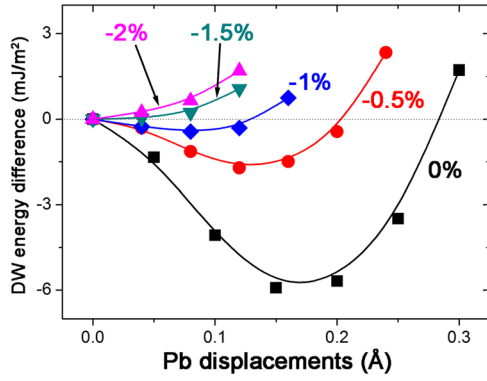


FIG. 3. The DW energy changes of DW-IB models relative to DW-I models when pushing Pb atoms at DWs at different strains.

and small compressive strains. The potential well depth decreases as the strain goes more compressive and disappears when the strain reaches  $-1.5\%$ , which means that the model DW-IB would become unstable compared with DW-I.

Based on these results obtained for the above DW-IB and DW-I models, full relaxations were performed to obtain the information on the DW-IBN and DW-IN models. Polarization analysis was done to the fully relaxed models, and the results are shown in Fig. 4. The larger the compressive strains are, the Ising components in the bulk area become larger and the slopes at the DW center become steeper. At the same time, the Bloch components shrink and disappear when the strain reaches  $-1.5\%$ , while the normal components increase continuously.

The decrease of Bloch components and the increase of Ising components can be easily understood by the coupling of polarization and strain: Epitaxial in-plane compressive strains should decrease the in-plane polarization (Bloch) and increase the out-of-plane polarization (Ising). However, we

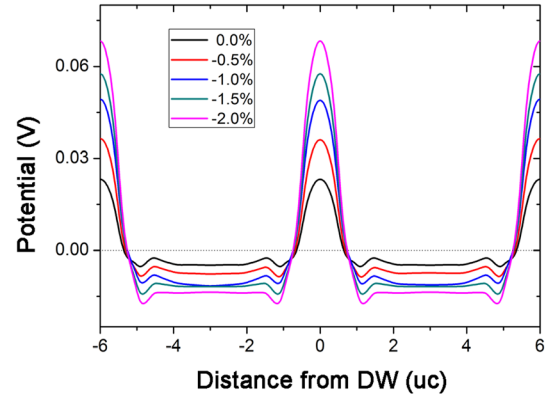


FIG. 5. The unit-cell-averaged potential distributions of  $180^\circ$  DWs at different epitaxial strains. The method to calculate the averaged potential is adopted from Ref. 7.

observed that normal components (also in-plane) increase with the increase of compressive strain [Fig. 4(c)]. The reason is that normal components mainly come from the elastic stress gradient due to the flexoelectric effect.<sup>14,31</sup> The elastic stress around the DW was found to be proportional to the square of  $P_3$  (Ising components),<sup>14,31</sup> whose gradient is definitely steeper at larger compressive strains [Fig. 4(a)]. According to our previous studies, the electronic origin of the flexoelectric effect at  $180^\circ$  DWs in tetragonal ferroelectrics is the non-uniform charge and potential distribution.<sup>32</sup> The potential at the DW area is higher than that at the bulk area, thus producing an electric field from the DW to the bulk, i.e., a tail-to-tail distribution around DWs. As a result, normal components also adopt a tail-to-tail distribution. Figure 5 gives the unit-cell-averaged potential distribution of the DW-I model at different epitaxial strains. As the strain becomes more compressive, the potential gradient becomes larger, which is the reason why normal components increase.

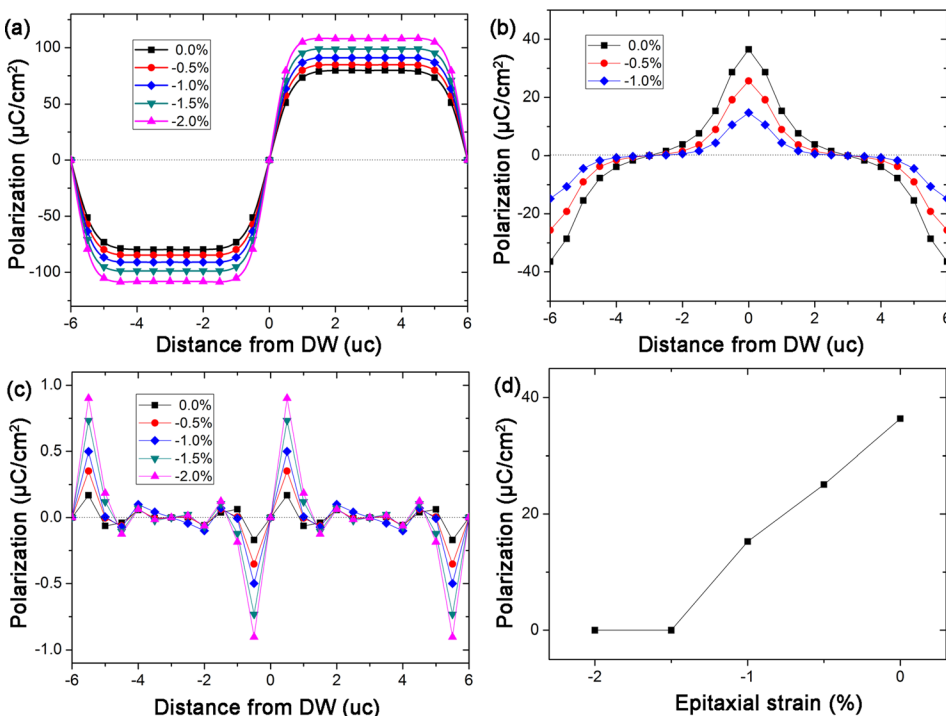


FIG. 4. The polarization distributions of Ising (a), Bloch (b), and normal (c) components at different strains. (d) The maximal Bloch component as the function of epitaxial strain.

#### IV. CONCLUSIONS

To sum up, we used first-principles calculations to study the effect of compressive strains on  $180^\circ$  DWs in ferroelectric PTO. It is found that compressive strains tend to decrease Bloch components and increase the Ising and normal components, inducing a chiral phase transition from a mixed Ising-Bloch type to a pure Ising type DW. The decrease and increase of these three components are found to be related to the polarization-strain-coupling and the flexoelectric effect. It is also found that the DW energy increases with increasing compressive strain. These results would provide useful information on the development of chiral-DW-based novel ferroelectric devices.

#### ACKNOWLEDGMENTS

This work was supported by the National Natural Science Foundation of China (Nos. 51401212, 51571197, 51231007, 51671194, and 51521091), the Doctoral Initiation Foundation of Liaoning Province (No. 20141144), National Basic Research Program of China (2014CB921002), and the Key Research Program of Frontier Sciences CAS (QYZDJ-SSW-JSC010).

- <sup>1</sup>A. K. Tagantsev, E. Courtens, and L. Arzel, *Phys. Rev. B* **64**, 224107 (2001).
- <sup>2</sup>Y. Gu, N. Wang, F. Xue, and L.-Q. Chen, *Phys. Rev. B* **91**, 174103 (2015).
- <sup>3</sup>L. Goncalves-Ferreira, S. A. T. Redfern, E. Artacho, and E. K. H. Salje, *Phys. Rev. Lett.* **101**, 097602 (2008).
- <sup>4</sup>S. Van Aert, S. Turner, R. Delville, D. Schryvers, G. Van Tendeloo, and E. K. H. Salje, *Adv. Mater.* **24**, 523 (2012).
- <sup>5</sup>X. K. Wei, A. K. Tagantsev, A. Kvasov, K. Roleder, C. L. Jia, and N. Setter, *Nat. Commun.* **5**, 3031 (2014).
- <sup>6</sup>W. Cao and L. E. Cross, *Phys. Rev. B* **44**, 5 (1991).
- <sup>7</sup>B. Meyer and D. Vanderbilt, *Phys. Rev. B* **65**, 104111 (2002).

- <sup>8</sup>D. Lee, R. Behera, P. Wu, H. Xu, Y. Li, S. B. Sinnott, S. Phillpot, L. Q. Chen, and V. Gopalan, *Phys. Rev. B* **80**, 060102 (2009).
- <sup>9</sup>R. K. Behera, C.-W. Lee, D. Lee, A. N. Morozovska, S. B. Sinnott, A. Asthagiri, V. Gopalan, and S. R. Phillpot, *J. Phys.: Condens. Matter* **23**, 175902 (2011).
- <sup>10</sup>J. Hlinka, V. Stepkova, P. Marton, I. Rychetsky, V. Janovec, and P. Ondrejko, *Phase Trans.* **84**, 738 (2011).
- <sup>11</sup>V. Stepkova, P. Marton, and J. Hlinka, *J. Phys.: Condens. Matter* **24**, 212201 (2012).
- <sup>12</sup>M. Taherinejad, D. Vanderbilt, P. Marton, V. Stepkova, and J. Hlinka, *Phys. Rev. B* **86**, 155138 (2012).
- <sup>13</sup>P. V. Yudin, A. K. Tagantsev, E. A. Eliseev, A. N. Morozovska, and N. Setter, *Phys. Rev. B* **86**, 134102 (2012).
- <sup>14</sup>Y. Gu, M. Li, A. N. Morozovska, Y. Wang, E. A. Eliseev, V. Gopalan, and L.-Q. Chen, *Phys. Rev. B* **89**, 174111 (2014).
- <sup>15</sup>M. Li, Y. Gu, Y. Wang, L.-Q. Chen, and W. Duan, *Phys. Rev. B* **90**, 054106 (2014).
- <sup>16</sup>Y. J. Wang, D. Chen, Y. L. Tang, Y. L. Zhu, and X. L. Ma, *J. Appl. Phys.* **116**, 224105 (2014).
- <sup>17</sup>J. Hlinka, V. Stepkova, P. Marton, and P. Ondrejko, in *Topological Structures in Ferroic Materials: Domain Walls, Vortices and Skyrmions*, edited by J. Seidel (Springer, 2016), Vol. 228, p. 163.
- <sup>18</sup>J. C. Wojdel and J. Íñiguez, *Phys. Rev. Lett.* **112**, 247603 (2014).
- <sup>19</sup>K. J. Choi *et al.*, *Science* **306**, 1005 (2004).
- <sup>20</sup>J. H. Haeni *et al.*, *Nature* **430**, 758 (2004).
- <sup>21</sup>Y. Li, S. Hu, Z. Liu, and L. Chen, *Acta Mater.* **50**, 395 (2002).
- <sup>22</sup>Y. L. Li, S. Choudhury, Z. K. Liu, and L. Q. Chen, *Appl. Phys. Lett.* **83**, 1608 (2003).
- <sup>23</sup>P. Marton, V. Stepkova, and J. Hlinka, *Phase Trans.* **86**, 103 (2013).
- <sup>24</sup>G. Kresse and J. Furthmüller, *Phys. Rev. B* **54**, 11169 (1996).
- <sup>25</sup>J. Hafner, *Comput. Phys. Commun.* **177**, 6 (2007).
- <sup>26</sup>J. Hafner, *J. Comput. Chem.* **29**, 2044 (2008).
- <sup>27</sup>P. E. Blochl, *Phys. Rev. B* **50**, 17953 (1994).
- <sup>28</sup>T. Shimada, Y. Umeno, and T. Kitamura, *Phys. Rev. B* **77**, 094105 (2008).
- <sup>29</sup>F. Jona and G. Shirane, *Ferroelectric Crystals* (Dover, New York, 1993).
- <sup>30</sup>R. D. King-Smith and D. Vanderbilt, *Phys. Rev. B* **47**, 1651 (1993); D. Vanderbilt and R. D. King-Smith, *ibid.* **48**, 4442 (1993); R. Resta, *Rev. Mod. Phys.* **66**, 899 (1994).
- <sup>31</sup>E. A. Eliseev, A. N. Morozovska, G. S. Svechnikov, P. Maksymovych, and S. V. Kalinin, *Phys. Rev. B* **85**, 045312 (2012).
- <sup>32</sup>Y. J. Wang, J. Y. Li, Y. L. Zhu, and X. L. Ma, e-print [arXiv:1709.06687](https://arxiv.org/abs/1709.06687).